Characterization of ionized gas outflows in low redshift star-forming galaxies

Guilherme S. Couto[*1], **Thomas Hughes**[2], **Médéric Boquien**[1], **Eduardo Ibar**[2]

[1] Centro de Astronomía (CITEVA), Universidad de Antofagasta, [2] Instituto de Física y Astronomía, Universidad de Valparaíso

* guilherme.couto@uantof.cl

Introduction

Galactic scale outflows are expected to play a major role in regulating the star formation [1,2], setting the observed masses of nearby early-type galaxies. Cosmological simulations invoke several mechanisms to regulate star formation, including wind launching and energy deposition related to supernovae. In this work we aim to shed light on the relation between galaxy evolution and stellar outflows, by characterizing the physical properties of a sample of low redshift galaxies using integral field spectrograph (IFS) data and spectral energy distribution (SED) modelling combined.

Data and Analysis

Our sample is composed of 15 main-sequence star-forming galaxies at $0.03 < z < 0.2$, a sub-sample from the Valparaíso ALMA Emission Line Survey (VALES, [3]). We used multi-wavelength data from the GAMA survey [4] for the analysis of the SED through the CIGALE code [5], and MUSE [6] IFS data to measure the ionized gas parameter such as integrated fluxes, peak velocities and velocity dispersions. This was performed measuring the emission lines after the subtraction of the stellar continuum using the STARLIGHT code [7] and the application of the Voronoi tessellation to increase the datacube S/N [8]. For the emission-lines measurements strategy, we initially fitted a single component Gaussian throughout the datacubes, and in regions where we detected residuals greater than 5 times the continuum noise, we add a second component, broader than the first, and redo the fit. This second component is interpreted to be related to outflowing gas.

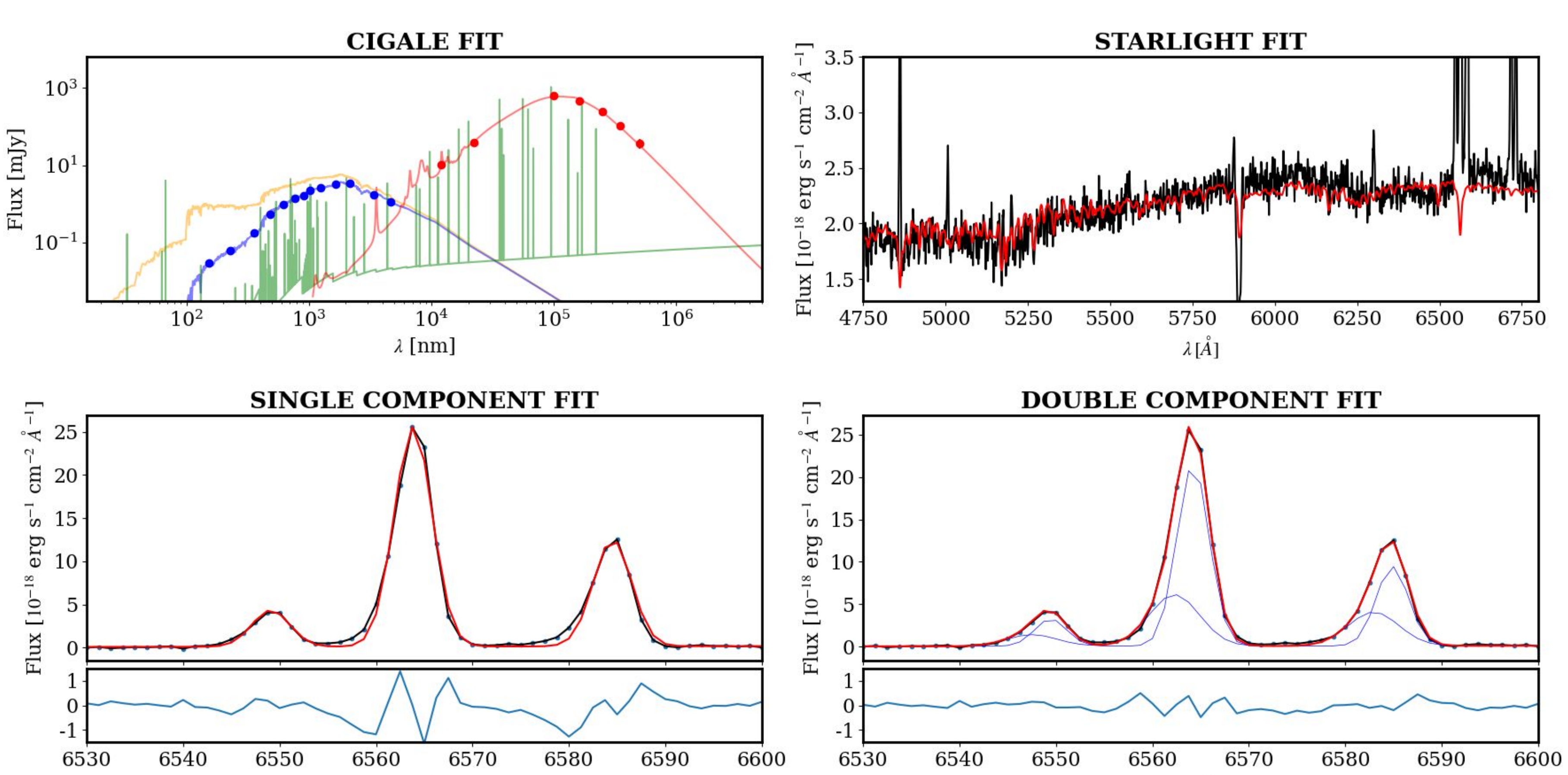

Fig. 1: Example of spectra fittings for one galaxy (HATLASJ083832). Top left: CIGALE SED fit, where points represent the GAMA survey data. Top right: STARLIGHT stellar continuum fit, with the black and red lines representing observed and modelled spectra, respectively. Bottom left: single-Gaussian fit ofthe Hα+[NII] emission lines. Bottom right: same as the previous panel, but showing the double-Gaussian fit.

Results

We used the emission-line measurements to analyze the outflow physical properties. In Fig. 2 we compare the observed line ratios to photoionization and shock models, coloring by the second component velocity dispersion. The photoionization models better reproduce the more turbulent gas, indicating that these are the earlier stages of the outflow, where shock-driven winds are still building up. Fig. 3 displays the dependence of the second component velocity dispersion, outflow velocity, outflow mass rate and mass loading factor ($\eta = \dot{M}_{out}/SFR$) with the SFR surface density. The former two parameters are probed with the Voronoi regions, while the latter two were obtained for the integrated outflowing area (the summed regions where we detect the second component). Correlations are observed for the former three parameters while the latter have a weak correlation but with a large scatter, thus a larger sample would be necessary to conclude in this relation. Low values of mass outflow rate and mass loading factor (median $\eta = 0.1$) are observed, indicating weak outflows. We also display in Fig. 4 the variation between the SFR at 100 and 10 Myr, obtained modelling the star formation histories with CIGALE, and its dependence with the integrated Hα ratio between the second and the first component, which indicate that the SFR is being suppressed in galaxies with increased outflow luminosity.

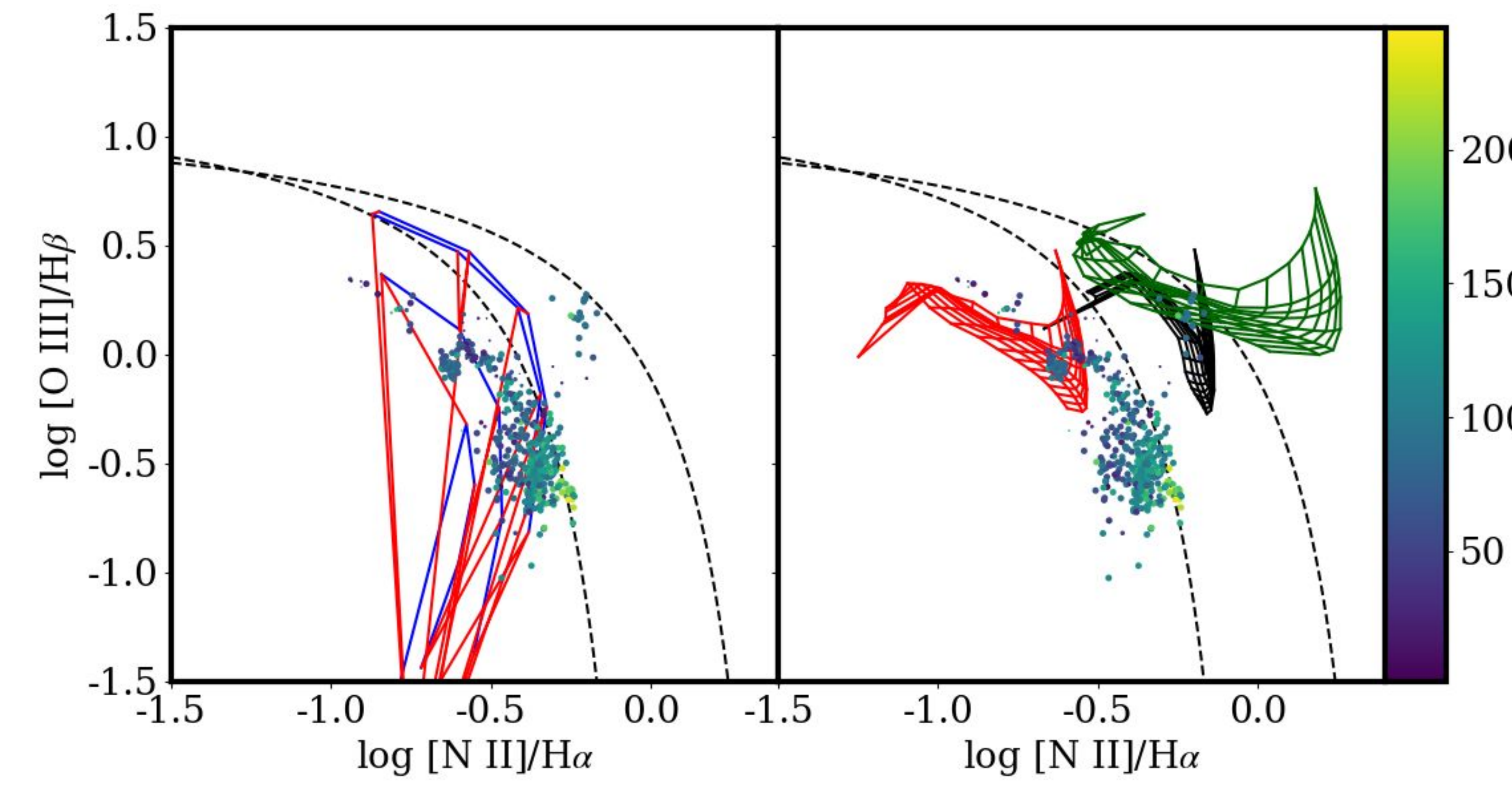

Fig. 2: BPT diagrams comparing the observed data (points colored with the second component velocity dispersion) with photoionization and shock models (left and right panels, respectively). We used the 3MdB database [9,10] obtained from Cloudy photoionization [11] and MAPPINGS V shocks [12] models. The blue and red lines in the left panel represent different stellar ages (1, 3, 4, 5.6 and 8.9x10^6 years) as ionization sources and different photoionization parameters ($-4.0 < \log(U) < -2.0$, in steps of 0.5), respectively. Red, black and green grids in the right panel are for LMC (Z=0.0071), Dopita_2005 (Z=0.0065) and Solar metallicities (Z=0.0183), respectively. Grids are for electron density $n_e = 1$ cm^{-3}, with magnetic fields $0.0001 < B < 10\mu G$ and shock velocities $100 < v_{shock} < 400$ km s^{-1}.

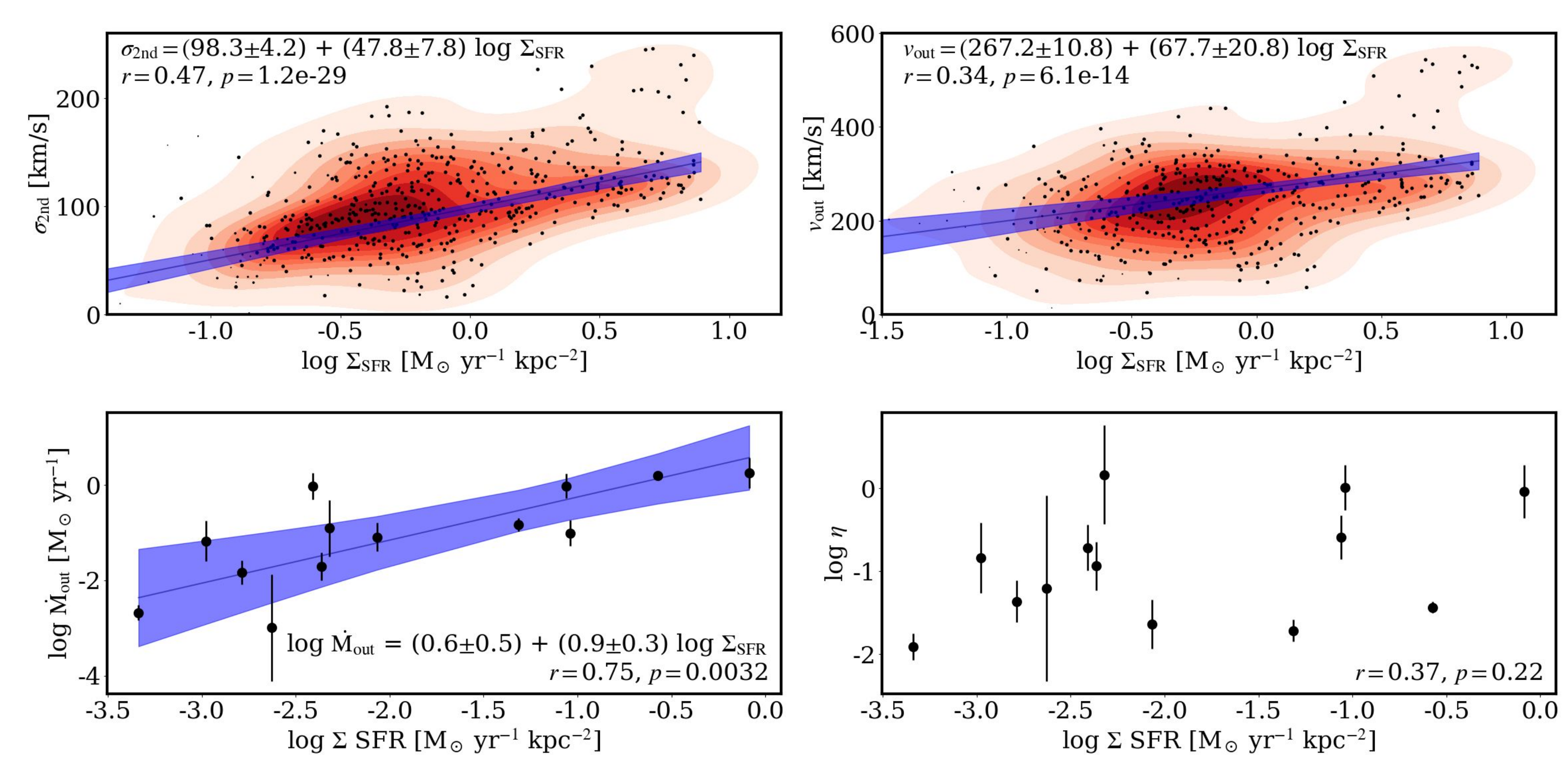

Fig. 3: Dependence of different outflow parameters with the SFR surface density. Top panels are probed using the Voronoi regions, while the bottom panels display the integrated outflow region for each galaxy. Best-fit correlations and Pearson coefficients are displayed in each panel.

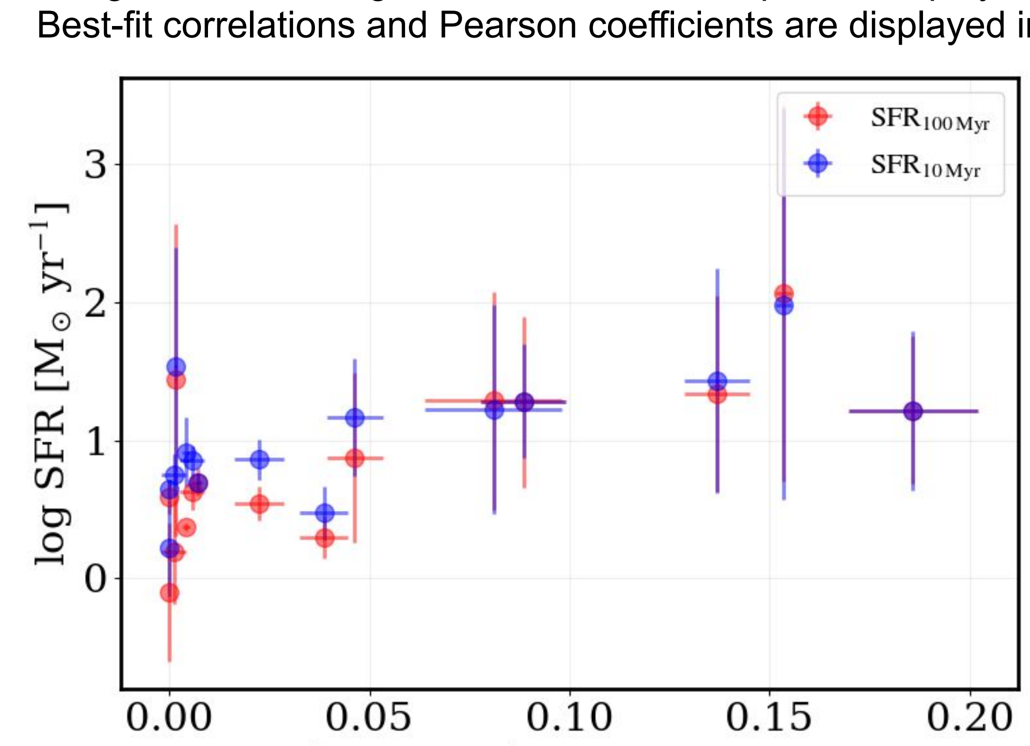

Fig. 4: SFR measured at 100 and 10 Myr as a dependence with the ratio between the integrated Hα luminosities of the second (outflowing gas) and first (star-forming gas) components. Points at the same x-axis value represent the same galaxy at different timescales.The SFR values were obtained through the SED modelling of the star formation history of each galaxy. The increase of SFR between 100 and 10 Myr period observed in galaxies showing low outflow luminosity contribution is not present in the galaxies showing higher outflow luminosities, indicating that the outflow is suppressing the most recent SFR.

- ★ **Weak gas outflows are observed tracing a second, broader component in our 15 star-forming galaxies sample.**
- ★ **Photoionization models better reproduce the observed line ratios when compared to shock-driven ionization models.**
- ★ **Outflow parameters such as velocity dispersion and mass outflow rate correlate with SFR surface density.**
- ★ **Galaxies with higher outflows contribution to Hα luminosity shows signature of SFR suppression in the recent (~10 Myr) timescales.**

References: [1] Hirschmann, M., Naab, T., Davé, R., et al., 2013, MNRAS, 436, 2929; [2] Chisholm, J., Tremonti, C. A., Leitherer, C., Chen, Y., 2017, MNRAS, 469, 4831; [3] Villanueva, V., Ibar, E., Hughes, T. M., et al. 2017, MNRAS, 470, 3775; [4] Driver, S. P., Wright, A. H., Andrews, S. K., et al. 2016, MNRAS, 455, 3911; [5] Boquien, M., Burgarella, D., Roehlly, Y., et al. 2019, A&A, 622, A103; [6] Bacon, R., Accardo, M., Adjali, L., et al. 2010, SPIE Conf. Ser., 7735, 8; [7] Cid Fernandes R., Mateus A., Sodré L., Stasińska G., Gomes J. M., 2005, MNRAS, 358, 363; [8] Cappellari, M., Copin, Y. 2003, MNRAS, 342, 345; [9] Morisset, C., Delgado-Inglada, G., Flores-Fajardo, N. 2015, Rev. Mexicana Astron. Astrofis., 51, 103; [10] Alarie, A. & Morisset, C. 2019, Rev. Astron. Astrofis., 55, 377; [11] Ferland, G. J., Porter, R. L., van Hoof, P. A. M., et al. 2013, Rev. Mexicana Astron. Astrofis., 49, 137; [12] Sutherland, R. S., Dopita, M. A. 2017, ApJS, 229, 34.